

Optical skyrmion lattices accelerating in free space

Haijun Wu,^{1,2} Weijie Zhou,² Zhihan Zhu,¹ and Yijie Shen^{2,3,*}

¹Wang Da-Heng Center, Heilongjiang Key Laboratory of Quantum Control,
Harbin University of Science and Technology, Harbin 150080, China

²Centre for Disruptive Photonic Technologies, School of Physical and Mathematical Sciences,
Nanyang Technological University, Singapore 637371, Singapore

³School of Electrical and Electronic Engineering,
Nanyang Technological University, Singapore 639798, Singapore

(Dated: January 10, 2025)

Generation and propagation of optical skyrmions provide a versatile platform for topologically nontrivial optical informatics and light-matter interactions, but their acceleration along curved trajectories is to be studied. In this study, we experimentally demonstrate the first accelerating skyrmion lattices conveyed by Airy structured light, characterized by topologically stable skyrmion textures with self-acceleration along parabolic trajectories. We show that the skyrmion unit cell can maintain a Skyrme number $|N_{\text{sk}}| > 0.9$ within a propagation range of $\pm 1.22 z_R$ upon parabolic acceleration. Notably, the meron structure remains $|N_{\text{sk}}|$ stable within 0.5 ± 0.02 over a significantly extended range of $\pm 3.06 z_R$. Our work provides a new potential carrier for topologically robust information distribution, particle sorting and manipulation.

INTRODUCTION

Optical skyrmions are a kind of vectorial structured light possessing nontrivial particle-like topologies [1]. Topological structures inherently bring protected stability in condensed matter physics [2–6], similar studies in optics are also emerging – topologies can make structured light robust against external perturbations [7–10]. Unlike the condensed-matter-based skyrmions localized in materials for potential data storage or local data processing [3–6], the optical skyrmions possess the ability to propagate in free space, which are invaluable for practical information transfer applications and nontrivial light-matter interaction [11–14]. Recently, exploiting advanced technologies of structured light modulation [15–17], both individual skyrmions and skyrmion lattices can be not only generated [18–21], but also propagating in free space with controlled topologies [22–27]. Especially, it becomes a mainstream to extend more complex topological structures controlled in higher dimensions, such as conformal skyrmion and meron lattices [28, 29], bimerons [30, 31], multiskyrmions and multimerons [32, 33], and hopfions [34–36], with more flexible control and resilient propagation. However, all the experimentally observed free-space skyrmions can only propagate straightly. Controlling topological skyrmions that spatially accelerate along curved trajectories is crucial for higher-level information sorting or transfer but remains a challenge.

In this work, we address this gap by demonstrating the generation of accelerating skyrmion lattices in paraxial beams and investigating their topological properties during propagation. Specifically, we generate paraxial skyrmion lattices through the non-separable superposition of orthogonally polarized Airy and vortex Airy beams. Through theoretical simulations and experimen-

tal verification, we show that the periodic Gaussian- and vortex-like intensity profiles of these beams naturally form skyrmion structures, which then evolve into stable skyrmion lattices. Furthermore, we demonstrate that the skyrmion and meron lattices maintain robust topological properties during free-space propagation, with stability observed over propagation ranges of $\pm 1.22 z_R$ and $\pm 3.06 z_R$, respectively, confirming their resilience under the influence of propagation effects. These findings highlight the potential of accelerating optical skyrmion lattices for future applications in topological information distribution, particle sorting and manipulation in nontrivial light-matter interactions, opening new directions in structured light research.

CONCEPT & PRINCIPLE

To better understand the optical skyrmion lattices described in this study, we first revisit the fundamental theory of skyrmions. The classic Néel-type skyrmion texture, as depicted in the inset of Fig. 1(a), is formed by unwrapping the vectors of a 3D parametric sphere onto a 2D transverse plane, resulting in a skyrmion structure represented by a 3D vector distribution $\mathbf{S}(x, y)$. Similarly, unwrapping hemispheres of the sphere forms meron textures, also analyzed in this study. Generally, for both skyrmion or meron textures, the topological invariant (times of the vector \mathbf{S} wraps around the sphere) is quantified by the Skyrme number [1]:

$$N_{\text{sk}} = \frac{1}{4\pi} \iint \mathbf{S} \cdot \left(\frac{\partial \mathbf{S}}{\partial x} \times \frac{\partial \mathbf{S}}{\partial y} \right) dx dy, \quad (1)$$

where the integrand $\rho_{\text{sk}} = \mathbf{S} \cdot (\partial_x \mathbf{S} \times \partial_y \mathbf{S})$ represents the skyrmie density.

Typically, optical skyrmions are created by the coherent combination of orthogonally polarized

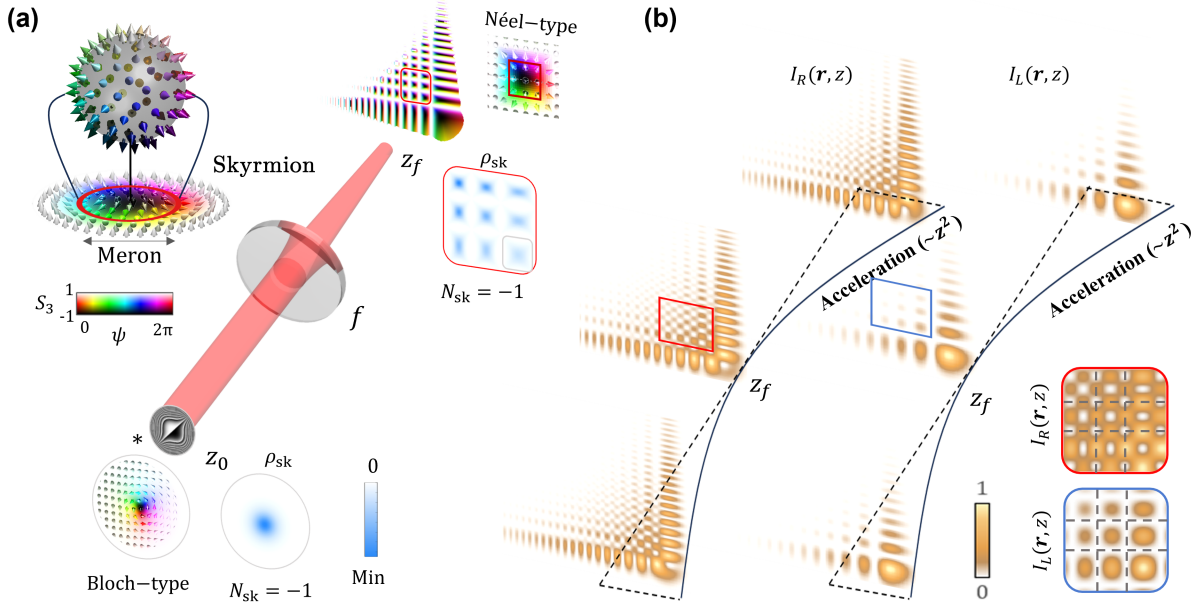


FIG. 1: **Concept of periodically accelerating skyrmion lattices.** **a**, Schematic of periodic skyrmion lattices generation via cubic phase modulation. The original Bloch-type skyrmion texture ($N_{\text{sk}} = -1$) transforms into square skyrmion lattices, each unit cell retaining $N_{\text{sk}} = -1$. The color map represents the Stokes vector orientation mapped to HSL color space, with maximum saturation. Hue encodes transverse orientation $\psi = \arg(S_1 + iS_2)$, and lightness corresponds to S_3 . **b**, Airy and vortex Airy beams, exhibiting periodic intensity lattices which complementary to each other (highlighted in red and blue regions), accelerate along curved trajectories.

Laguerre-Gaussian (LG) beams with different topological charges [37]. The field distribution is given by:

$$\mathbf{E}(x, y) = \sqrt{\alpha} \text{LG}_{\ell_1, 0}(x, y) \hat{\mathbf{e}}_R + e^{i\theta} \sqrt{1 - \alpha} \text{LG}_{\ell_2, 0}(x, y) \hat{\mathbf{e}}_L \quad (2)$$

where, $\alpha \in [0, 1]$ defines the relative amplitude of the two modes, and $\text{LG}_{\ell, p}$ represents the LG mode with azimuthal and radial indices ℓ and p , respectively (see **Supplementary Material S1** for detailed expressions). Here, $|\ell_1| \neq |\ell_2|$, and $e^{i\theta}$ determines the intramodal phase, which governs the skyrmion state, and $\hat{\mathbf{e}}_R$ and $\hat{\mathbf{e}}_L$ are unit vectors of right-circular polarization (RCP) and left-circular polarization (LCP). By modulating the parameters in Eq. (1), we can construct the distribution of normalized Stokes vector $\mathbf{S}(x, y) = [S_1(x, y), S_2(x, y), S_3(x, y)]^T$, which describes the 3D vector distribution of optical topological textures [23].

Returning to the main focus, A natural route to construct accelerating skyrmion lattices leverages the unique properties of Airy beams, which exhibit non-diffracting, self-accelerating intensity distributions with periodic lattice structures in the transverse plane [38, 39]. While ideal Airy beams require infinite energy, finite-energy Airy beams can be realized through the Fourier transform of a Gaussian beam modulated by a cubic phase. Introducing vortex phases during this process results in vortex Airy beams, which generate periodic vortex lattices com-

plementary to the original Airy intensity distribution due to spiral phase contrast (see **Supplementary Material S2** for more details) [40–42]. Thus, the skyrmion lattices in this work can be described as:

$$\begin{aligned} \mathbf{E}_T(x_0, y_0) &= \mathcal{F} \left[\mathbf{E}(x, y) \exp \left(\frac{ib^3 (x^3 + y^3)}{3} \right) \right] \quad (3) \\ &= \sqrt{\alpha} A_{\ell_1}(x_0, y_0) \hat{\mathbf{e}}_R + e^{i\theta} \sqrt{1 - \alpha} A_{\ell_2}(x_0, y_0) \hat{\mathbf{e}}_L \end{aligned}$$

Where, $A_{\ell}(\cdot)$ is vortex Airy beam converted by topological charge ℓ , and b is the scaling factor of the Airy function determining the rate of transverse acceleration. This process is shown as Fig. 1(a), for $\ell_1 = 1$, $\ell_2 = 0$ and $\theta = -\pi/2$, the skyrmion texture gradually evolves into periodic skyrmion lattices at the Fourier plane, displaying square symmetry in their unit cells. Despite the geometric transformation, the Skyrmie number for each cell remains $N_{\text{sk}} = -1$, equivalent to the original circular skyrmions.

The transition between Bloch-type and Néel-type skyrmion textures at different propagation planes (z_0 to z_f) is attributed to the accumulation of Gouy phase, which varies with the spatial mode order [43]. As shown in Fig. 1(b), during propagation, both Airy and vortex Airy beams exhibit 3D intensity profiles that accelerate along parabolic trajectories, transferring their self-accelerating behavior to the constructed skyrmion lattices. This mechanism enables the skyrmion lattices to

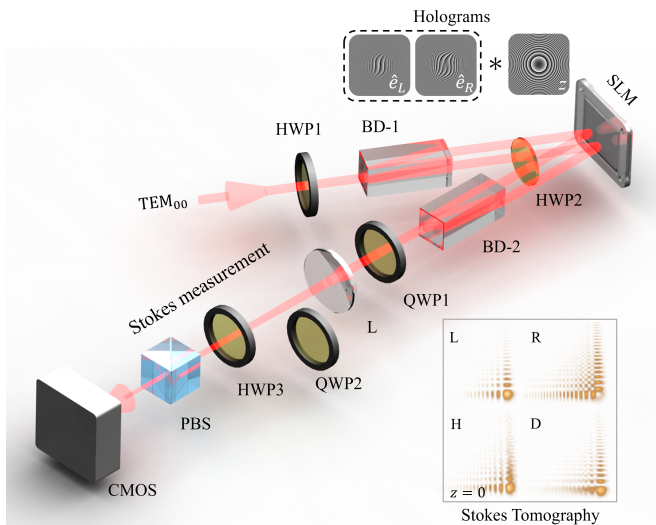


FIG. 2: **Experimental setup.** The key components include, beam displacer prisms (BD), spatial light modulator (SLM), a camera (CMOS), half-wave plate (HWP), quarter-wave plate (QWP).

maintain their topological structures within a specific propagation range, ensuring stability and robustness.

EXPERIMENTAL SETUP

To further demonstrate the accelerating properties of skyrmion lattices, the experimental setup is depicted in Fig. 2. A self-locking polarization Mach-Zehnder interferometer, incorporating two beam displacers (BD-1 and BD-2), forms the core of the system. A continuous 532 nm TEM_{00} laser beam (CNI Laser MSL-III-532) passes through BD-1, splitting into two orthogonally polarized beams directed to separate regions of a spatial light modulator (SLM, Holoeye ERIS-NIR-153). These beams are individually modulated using complex amplitude modulation (CAM) holograms corresponding to the Fourier transforms of the desired Airy and vortex Airy beams [44]. The beam radius w_0 and scaling factor b are set as to 1 mm and $\sqrt[3]{3/11}$, respectively. A half-wave plate (HWP2, fixed at 45°) ensures horizontal polarization for both beams before modulation by the SLM. After modulation, BD-2 recombines the beams. A quarter-wave plate (QWP1, fixed at 45°) and a Fourier lens (L) with a focal length of 200 mm are used to reconstruct the Airy vector beam at the Fourier plane. The propagation tomographies of the Airy beams are recorded via a digital propagation technique integrated into the CAM holograms, eliminating the need for physical translation of the CMOS camera (Allied Vision Alvium 1800 U-240m) along the z -axis [45, 46]. Furthermore, the camera, combined with polarizers (QWP2, HWP3, and PBS), performs spatial Stokes tomography, capturing the struc-

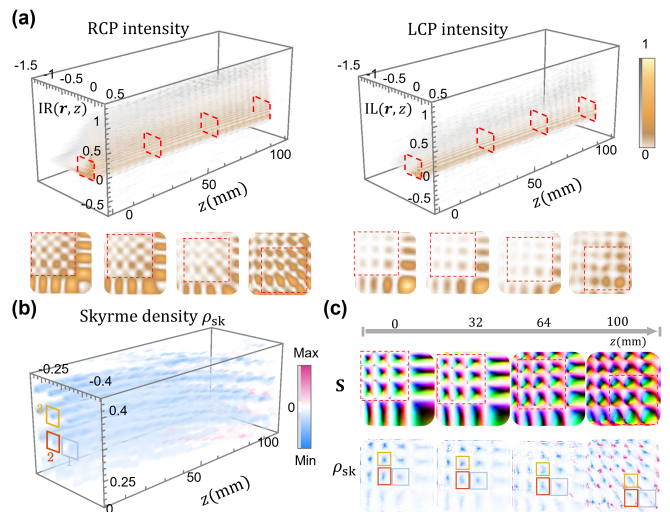


FIG. 3: **Experimental results for periodically accelerating skyrmion lattices.** **a**, 3D intensity profiles of vortex Airy (RCP) and Airy (LCP) beams, reconstructed from experimental measurements, with selectively sampled transverse intensity lattices at different propagation distances (0 mm, 32 mm, 64 mm, and 100 mm). **b**, 3D skyrmion density distributions corresponding to the self-accelerating intensity lattices. **c**, Detailed distributions of the Stokes vector and skyrmion density at different z planes. As propagation distance increases, skyrmion textures degrade, and positive ρ_{sk} values (red) gradually emerge alongside the initially negative ρ_{sk} lattices (blue).

tures of skyrmion lattices in Stokes space.

RESULTS & DISCUSSION

Fig. 3(a) shows the observed 3D profiles of vortex Airy (RCP) and Airy (LCP) beams (reconstructed from 26 slices) with a Rayleigh length of $z_R = 32.701$ mm, where both components propagate along diagonal curved trajectories (see **Supplementary Material S2** for more details). Transverse intensity profiles below the 3D profiles reveal periodic lattice structures that degrade with propagation, more prominently for vortex Airy beams. At $z = 100$ mm, vortex lattices even become indistinguishable. The corresponding 3D skyrmion density distributions are presented in Fig. 3(b). At the Fourier plane ($z = 0$), perfectly periodic Stokes vector and skyrmion density distributions are observed (Fig. 3(c)). However, as propagation distance increases, vortex lattice degradation leads to skyrmion cell deformation, a shrinking $S_3 = 1$ area, and the emergence of abnormal positive ρ_{sk} values (Theoretical references for these results are provided in Fig. S3). This raises an important question: how stable are the topological structures during propagation?

To quantify the stability, the skyrmion numbers of three cells of skyrmion lattices (labeled 1, 2, and 3) were calcu-

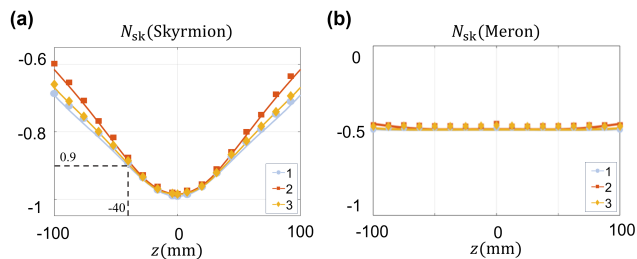


FIG. 4: **Quantitative analysis of accelerating skyrmion and meron lattices.** **a**, Skyrmion number for skyrmion lattices, showing a gradual decrease with propagation distance. **b**, skyrmion number for meron lattices, remaining stable over propagation distance. Point data correspond to experimental observations, and solid lines represent theoretical results.

lated, as shown in Fig. 4(a). As the lattices degrade, the skyrmion number N_{sk} gradually decreases with distance, with cell 2 showing the fastest decline due to its smaller integration area, which becomes insufficient for maintaining accuracy with increasing lattice complexity. Despite these challenges, skyrmion lattices maintain stable acceleration over a range of ± 40 mm ($\pm 1.22 z_R$), with $|N_{sk}| > 0.9$. Beyond this range, N_{sk} drops to approximately -0.6.

Interestingly, meron lattices, which occupy the core regions of skyrmion structures, demonstrate a greater level of robustness. As shown in Fig. 4(b), meron lattices maintain stability across the entire measured range ($\pm 3.06 z_R$), with $N_{sk} \approx -0.5$, as shown in Fig. 4(b). This stability is achieved at the expense of reduced $S_3 = 1$ regions, as the inner topological structures are better preserved.

Overall, Skyrmion lattices in this work not only inherit the stable acceleration and self-healing properties of Airy beams [47–49] (see **Supplementary Material S3** for details of self-healing) but also introduce an additional degree of freedom due to their intricate topological structures. These features not only unlock new opportunities for exploring their dynamic behavior but also show promise for practical applications.

CONCLUSION

We have experimentally demonstrated a versatile family of optical skyrmion lattices capable of accelerating along curved trajectories in free space. These lattices are generated by imprinting cubic phase modulation onto traditional skyrmion beams. The transverse acceleration rate of these trajectories can be flexibly controlled by adjusting the scaling factor b . Importantly, only LG beams that form skyrmion structures with odd topological charge differences can generate skyrmion lattices.

Leveraging the non-diffracting and self-accelerating na-

ture of Airy beams, skyrmion lattices exhibit stable transverse acceleration and robust topological properties over a propagation range of $\pm 1.22 z_R$, even under propagation-induced lattice deformation. Greater robustness is observed for Meron lattices, which occupy the core regions of skyrmion structures and remain stable over an extended range of $\pm 3.06 z_R$.

These unique features establish skyrmion lattices as a promising platform for exploring advanced applications such as particle sorting [50–52], advanced microscopy [51–56], plasma channel induction [51, 57], electron beam manipulation [51, 52], and guiding electric discharges [58], opening new frontiers in structured light research.

SUPPLEMENTARY MATERIAL

See supplementary material for more details of Laguerre-Gaussian Modes, Airy and vortex Airy beams.

Singapore Ministry of Education (MOE) AcRF Tier 1 grant (RG157/23), MoE AcRF Tier 1 Thematic grant (RT11/23), and Imperial-Nanyang Technological University Collaboration Fund (INCF-2024-007), Nanyang Technological University Start Up Grant, and National Natural Science Foundation of China (12474324, 62075050, 11934013).

Data Availability Statement

The data that support the findings of this study are available from the corresponding author upon reasonable request.

* Electronic address: yijie.shen@ntu.edu.sg

- [1] Shen, Y. *et al.* Optical skyrmions and other topological quasiparticles of light. *Nature Photonics* **18**, 15–25 (2024).
- [2] Bernevig, B. A., Felser, C. & Beidenkopf, H. Progress and prospects in magnetic topological materials. *Nature* **603**, 41–51 (2022).
- [3] Bogdanov, A. N. & Panagopoulos, C. Physical foundations and basic properties of magnetic skyrmions. *Nature Reviews Physics* **2**, 492–498 (2020).
- [4] Fert, A., Reyren, N. & Cros, V. Magnetic skyrmions: advances in physics and potential applications. *Nature Reviews Materials* **2**, 1–15 (2017).
- [5] Han, L. *et al.* High-density switchable skyrmion-like polar nanodomains integrated on silicon. *Nature* **603**, 63–67 (2022).
- [6] Chen, S. *et al.* All-electrical skyrmionic magnetic tunnel junction. *Nature* **627**, 522–527 (2024).
- [7] Wang, A. A. *et al.* Topological protection of optical skyrmions through complex media. *Light: Science & Applications* **13**, 314 (2024).

- [8] Liu, C., Zhang, S., Maier, S. A. & Ren, H. Disorder-induced topological state transition in the optical skyrmion family. *Physical Review Letters* **129**, 267401 (2022).
- [9] Wang, R. *et al.* Observation of resilient propagation and free-space skyrmions in toroidal electromagnetic pulses. *Applied Physics Reviews* **11** (2024).
- [10] Ornelas, P., Nape, I., de Mello Koch, R. & Forbes, A. Non-local skyrmions as topologically resilient quantum entangled states of light. *Nature Photonics* **18**, 258–266 (2024).
- [11] Wan, Z., Wang, H., Liu, Q., Fu, X. & Shen, Y. Ultra-degree-of-freedom structured light for ultracapacity information carriers. *ACS Photonics* **10**, 2149–2164 (2023).
- [12] Wang, R. *et al.* Single-antenna super-resolution positioning with nonseparable toroidal pulses. *Communications Physics* **7**, 356 (2024).
- [13] Habibović, D., Hamilton, K. R., Neufeld, O. & Rego, L. Emerging tailored light sources for studying chirality and symmetry. *Nature Reviews Physics* 1–13 (2024).
- [14] Tamura, R. *et al.* Direct imprint of optical skyrmions in azopolymers as photoinduced relief structures. *APL Photonics* **9** (2024).
- [15] Forbes, A., Oliveira, M. & Dennis, M. Structured light. *Nature Photonics* **15**, 253–262 (2021).
- [16] He, C., Shen, Y. & Forbes, A. Towards higher-dimensional structured light. *Light: Science & Applications* **11**, 205 (2022).
- [17] Rosales-Guzmán, C. & Rodríguez-Fajardo, V. A perspective on structured light’s applications. *Applied Physics Letters* **125** (2024).
- [18] Tsesses, S. *et al.* Optical skyrmion lattice in evanescent electromagnetic fields. *Science* **361**, 993–996 (2018).
- [19] Du, L., Yang, A., Zayats, A. V. & Yuan, X. Deep-subwavelength features of photonic skyrmions in a confined electromagnetic field with orbital angular momentum. *Nature Physics* **15**, 650–654 (2019).
- [20] Davis, T. J. *et al.* Ultrafast vector imaging of plasmonic skyrmion dynamics with deep subwavelength resolution. *Science* **368** (2020).
- [21] Dai, Y. *et al.* Plasmonic topological quasiparticle on the nanometre and femtosecond scales. *Nature* **588**, 616–619 (2020).
- [22] Gao, S. *et al.* Paraxial skyrmionic beams. *Physical Review A* **102**, 053513 (2020).
- [23] Shen, Y., Martínez, E. C. & Rosales-Guzmán, C. Generation of optical skyrmions with tunable topological textures. *ACS Photonics* **9**, 296–303 (2022).
- [24] Hakobyan, V., Shen, Y. & Brasselet, E. Unitary spin-orbit optical-skyrmionic wave plates. *Physical Review Applied* **22**, 054038 (2024).
- [25] He, T. *et al.* Optical skyrmions from metafibers with sub-wavelength features. *Nature Communications* **15**, 10141 (2024).
- [26] Kerridge-Johns, W. R., Rao, A. S. & Omatsu, T. Optical skyrmion laser using a wedged output coupler. *Optica* **11**, 769–775 (2024).
- [27] Lin, W., Ota, Y., Arakawa, Y. & Iwamoto, S. On-chip optical skyrmionic beam generators. *Optica* **11**, 1588–1594 (2024).
- [28] Marco, D., Herrera, I., Brasselet, S. & Alonso, M. A. Propagation-invariant optical meron lattices. *ACS Photonics* (2024).
- [29] Marco, D., Herrera, I., Brasselet, S. & Alonso, M. A. Periodic skyrmionic textures via conformal cartographic projections. *APL Photonics* **9** (2024).
- [30] Shen, Y. Topological bimeronic beams. *Optics Letters* **46**, 3737–3740 (2021).
- [31] Berškys, J. & Orlov, S. Accelerating airy beams with particle-like polarization topologies and free-space bimeronic lattices. *Optics letters* **48**, 1168–1171 (2023).
- [32] Shen, Y. *et al.* Topologically controlled multiskyrmions in photonic gradient-index lenses. *Physical Review Applied* **21**, 024025 (2024).
- [33] McWilliam, A. *et al.* Topological approach of characterizing optical skyrmions and multi-skyrmions. *Laser & Photonics Reviews* **17**, 2300155 (2023).
- [34] Shen, Y. *et al.* Topological transformation and free-space transport of photonic hopfions. *Advanced Photonics* **5**, 015001 (2023).
- [35] Sugic, D. *et al.* Particle-like topologies in light. *Nature communications* **12**, 1–10 (2021).
- [36] Tamura, R., Allam, S. R., Litchinitser, N. M. & Omatsu, T. Three-dimensional projection of optical hopfion textures in a material. *ACS Photonics* (2024).
- [37] Allen, L., Beijersbergen, M. W., Spreeuw, R. & Woerdman, J. Orbital angular momentum of light and the transformation of laguerre-gaussian laser modes. *Physical review A* **45**, 8185 (1992).
- [38] Efremidis, N. K., Chen, Z., Segev, M. & Christodoulides, D. N. Airy beams and accelerating waves: an overview of recent advances. *Optica* **6**, 686–701 (2019).
- [39] Shi, Z., Xue, J., Zhu, X., Xiang, Y. & Li, H. Interaction of airy-gaussian beams in photonic lattices with defects. *Physical Review E* **95**, 042209 (2017).
- [40] Dai, H., Liu, Y., Luo, D. & Sun, X. Propagation dynamics of an optical vortex imposed on an airy beam. *Optics letters* **35**, 4075–4077 (2010).
- [41] Qiu, X., Li, F., Zhang, W., Zhu, Z. & Chen, L. Spiral phase contrast imaging in nonlinear optics: seeing phase objects using invisible illumination. *Optica* **5**, 208–212 (2018).
- [42] Pan, J., Wang, H., Shen, Y., Fu, X. & Liu, Q. Airy coherent vortices: 3d multilayer self-accelerating structured light. *Applied Physics Letters* **121** (2022).
- [43] Zhong, R.-Y. *et al.* Gouy-phase-mediated propagation variations and revivals of transverse structure in vectorially structured light. *Physical Review A* **103**, 053520 (2021).
- [44] Rosales-Guzmán, C. & Forbes, A. How to shape light with spatial light modulators (Society of Photo-Optical Instrumentation Engineers (SPIE), 2017).
- [45] Osten, W. *et al.* Recent advances in digital holography. *Applied optics* **53**, G44–G63 (2014).
- [46] Schulze, C., Flamm, D., Duparré, M. & Forbes, A. *Beam-quality measurements using a spatial light modulator* (Optical Society of America, 2012).
- [47] Chu, X., Zhou, G. & Chen, R. Analytical study of the self-healing property of airy beams. *Physical Review A—Atomic, Molecular, and Optical Physics* **85**, 013815 (2012).
- [48] Broky, J., Siviloglou, G. A., Dogariu, A. & Christodoulides, D. N. Self-healing properties of optical airy beams. *Optics express* **16**, 12880–12891 (2008).
- [49] Zhang, L. *et al.* Investigating the self-healing property of an optical airy beam. *Optics Letters* **40**, 5066–5069 (2015).
- [50] Baumgartl, J., Mazilu, M. & Dholakia, K. Optically me-

- diated particle clearing using airy wavepackets. *Nature photonics* **2**, 675–678 (2008).
- [51] Schley, R. *et al.* Loss-proof self-accelerating beams and their use in non-paraxial manipulation of particles' trajectories. *Nature communications* **5**, 5189 (2014).
 - [52] Voloch-Bloch, N., Lereah, Y., Lilach, Y., Gover, A. & Arie, A. Generation of electron airy beams. *Nature* **494**, 331–335 (2013).
 - [53] Jia, S., Vaughan, J. C. & Zhuang, X. Isotropic three-dimensional super-resolution imaging with a self-bending point spread function. *Nature photonics* **8**, 302–306 (2014).
 - [54] Vettenburg, T. *et al.* Light-sheet microscopy using an airy beam. *Nature methods* **11**, 541–544 (2014).
 - [55] Nylk, J. *et al.* Light-sheet microscopy with attenuation-compensated propagation-invariant beams. *Science advances* **4**, eaar4817 (2018).
 - [56] Wang, J., Hua, X., Guo, C., Liu, W. & Jia, S. Airy-beam tomographic microscopy. *Optica* **7**, 790–793 (2020).
 - [57] Polynkin, P., Kolesik, M., Moloney, J. V., Siviloglou, G. A. & Christodoulides, D. N. Curved plasma channel generation using ultraintense airy beams. *Science* **324**, 229–232 (2009).
 - [58] Clerici, M. *et al.* Laser-assisted guiding of electric discharges around objects. *Science advances* **1**, e1400111 (2015).